

Haruo Sato · Michael C. Fehler
Takuto Maeda

Seismic Wave Propagation and Scattering in the Heterogeneous Earth

Second Edition

 Springer

Seismic Wave Propagation and Scattering
in the Heterogeneous Earth: Second Edition

Haruo Sato • Michael C. Fehler
Takuto Maeda

Seismic Wave Propagation and Scattering in the Heterogeneous Earth: Second Edition

 Springer

Prof. Haruo Sato
Dept. of Geophysics
Graduate School of Science
Tohoku University
Aramaki-Aza-Aoba 6-3, Aoba-ku
Sendai-shi, Miyagi-ken 980-8578
Japan
sato@zisin.gp.tohoku.ac.jp

Dr. Michael C. Fehler
Dept. of Earth, Atmospheric and
Planetary Sciences
Earth Resources Laboratory
Massachusetts Institute of Technology
77 Massachusetts Ave.
Cambridge, Massachusetts 02139
USA
fehler@mit.edu

Dr. Takuto Maeda
Center for Integrated Disaster
Information Research
Interfaculty Initiative in Information Studies
The University of Tokyo
Yayoi 1-1-1, Bunkyo-ku
Tokyo-to 113-0032
Japan
maeda@eri.u-tokyo.ac.jp

ISBN 978-3-642-23028-8 e-ISBN 978-3-642-23029-5
DOI 10.1007/978-3-642-23029-5
Springer Heidelberg Dordrecht London New York

Library of Congress Control Number: 2011945604

© Springer-Verlag Berlin Heidelberg 2012

This work is subject to copyright. All rights are reserved, whether the whole or part of the material is concerned, specifically the rights of translation, reprinting, reuse of illustrations, recitation, broadcasting, reproduction on microfilm or in any other way, and storage in data banks. Duplication of this publication or parts thereof is permitted only under the provisions of the German Copyright Law of September 9, 1965, in its current version, and permission for use must always be obtained from Springer. Violations are liable to prosecution under the German Copyright Law.

The use of general descriptive names, registered names, trademarks, etc. in this publication does not imply, even in the absence of a specific statement, that such names are exempt from the relevant protective laws and regulations and therefore free for general use.

Printed on acid-free paper

Springer is part of Springer Science+Business Media (www.springer.com)

*Dedicated to
Keiiti Aki (1930–2005)
Inspired Mentor and Pioneer of Modern Seismology*

Preface to the Second Edition

Scattering due to randomly distributed small-scale heterogeneities in the earth significantly changes seismic waveforms of local earthquakes especially for short periods. Scattering excites long lasting coda waves after the direct arrival and broadens the apparent duration of oscillation with increasing travel distance much longer than the source duration time. Models of propagation through deterministic structures such as those with horizontally uniform velocity layers cannot explain those observed phenomena. Our goal in writing this book is to put a focus on the phenomena of seismic wave scattering by distributed heterogeneities in the earth, especially in the lithosphere, where stochastic treatment is essential to describe both heterogeneous media and wave propagation through them. Stochastic approaches and deterministic approaches are complementary for the construction of a unified image of the earth's structure.

Keiiti Aki was a distinguished pioneer who extensively developed various stochastic methods for short-period seismology. His strong encouragement and continuous support for us were essential in motivating us to write the first edition of this book. Before Kei passed away in 2005, he kindly cited our book when he argued for the importance of the study on seismic wave scattering caused by small-scale heterogeneity in his letter to V. I. Keilis-Borok, "... To a geodynamicist, the earth's property is smoothly varying within bodies bounded by large-scale interfaces. Most seismologists also belong to this "smooth earth club," because once you start with an initial model of smooth earth your data usually do not require the addition of small-scale heterogeneity to your initial model. As summarized well in a recent book by [Sato and Fehler \(1998\)](#), the acceptance of coda waves in the data set is needed for the acceptance of small-scale seismic heterogeneity of the lithosphere. There are an increasing number of seismologists who accept it, forming the "rough earth club." I believe that you are also a member of the rough earth club, judging from the emphasis on the hierarchical heterogeneity of the lithosphere. ..."(Aki 2009).

The first edition of this book was fortunately accepted in the geophysical community as a textbook, especially for graduate students. Furthermore it has been often cited in the physics community since this book introduced various aspects of wave scattering in real heterogeneous media. During the decade following the

publication of the first edition, there were developments in stochastic methods and analyses focusing on seismogram envelopes. Radiative transfer theory has been used not only for the study of coda envelopes but also for the analysis of whole seismogram envelopes. These studies made it possible to resolve the spatial variation of scattering strength. There have been developments in the statistical description of wave propagation in random media that reliably predict the delay of peak amplitude from the onset and the broadening of seismogram envelopes with increasing travel distance. Those methods have also been extended from scalar waves to vector waves. Investigators from throughout the world participated and collaborated in these developments as members of the IASPEI task group on “Scattering and Heterogeneity,” of which the summary was published in [Sato and Fehler \(2008\)](#).

In 2008, we started to write the second edition of this book. We expanded from the first edition by introducing recent developments in theory and analysis, updated illustrations and references, and wrote more precise steps in mathematical equations. The radiative transfer theory chapter and the Markov approximation chapter have been enlarged. We added two newly created chapters; one is a bridge between wave propagation in random media and the radiative transfer theory and the other one is on the Green’s function retrieval from the cross-correlation function of ambient noise.

We would like to express our sincere gratitude to the following colleagues and ex-graduate students for their collaboration and fruitful discussions: M. Korn, R.S. Wu, M. Ohtake, A. Jin, T. Nishimura, H. Nakahara, K. Yoshimoto, M. Yamamoto, O. Nishizawa, S. Kinoshita, T. Yamashita, K. Yomogida, S. Matsumoto, J. Kawahara, M. Hoshiya, K. Obara, K. Nishigami, N. Uchida, T.W. Chung, T. Saito, U. Wegler, L. Margerin, M. Campillo, G. Poupinet, R. Snieder, L.J. Hunag, M. Nishino, Y. Fukushima, K. Shiomi, T. Takahashi, K. Lee, W.S. Lee, M. Kubanza, K. Sawazaki, E. Carcole, J. Tripathi, N. Takagi, K. Emoto, H. Zhang, Y. Asano, H. Kumagai, T. Furumura, T. Matsuzawa, T. Ueno, S. Padhy, S. Takemura, T. Takemoto and H. Asano. Special thanks to National Research Institute for Earth Science and Disaster Prevention, Japan for kind permission for us to use digital seismograms of their networks.

*Haruo Sato
Michael C. Fehler
Takuto Maeda*

Preface to the First Edition

The structure of the earth has been extensively studied using seismic waves generated by natural earthquakes and manmade sources. In classical seismology, the earth is considered to consist of a sequence of horizontal layers having differing elastic properties, which are determined from travel-time readings of body waves and the dispersion of surface waves. More recently, three-dimensional inhomogeneity having scale larger than the predominant seismic wavelength has been characterized using travel-time data with velocity tomography. Forward and inverse waveform modeling methods for deterministic models have been developed that can model complicated structures allowing many features of complex waveforms to be successfully explained. Classical seismic methods are described in books like *Quantitative Seismology: Theory and Methods* by [Aki and Richards \(1980\)](#), *Seismic Waves and Sources* by [Ben-Menahem and Singh \(1981\)](#), *Theory and Application of Microearthquake Networks* by [Lee and Stewart \(1981\)](#), *Seismic Wave Propagation in Stratified Media* by [Kennett \(1985\)](#), and *Modern Global Seismology* by [Lay and Wallace \(1995\)](#). High-frequency (>1 Hz) seismograms of local earthquakes, however, often contain continuous wave trains following the direct S-wave that cannot be explained by the deterministic structures developed from tomographic or other methods. Array observations have shown that these wave trains, known as “coda waves,” are incoherent waves scattered by randomly distributed heterogeneities having random sizes and contrasts of physical properties. The characteristic scale of the heterogeneity that has the most influence on a given wave is not always much longer than but is usually the same order of the wavelength of the seismic wave. Strong random fluctuations in seismic velocity and density having short wavelengths superposed on a step-like structure are found in well-logs of boreholes drilled even in old crystalline rocks located in stable tectonic environments. These observations suggest a description of the earth as a random medium with a broad spectrum of spatial velocity fluctuations and the resulting importance of seismic wave scattering.

In the 1970s, geophysicists began to investigate the relationship between seismogram envelopes and the spectral structure of the random heterogeneity in the earth. Initial models were based on a phenomenological description of the scattering

process. Later, in parallel with additional observational work, there have been theoretical studies using perturbation methods, the parabolic approximation, the phase screen method, and another phenomenological method known as the radiative transfer theory. These developments have gradually established a description of the scattering process of seismic waves in the inhomogeneous earth and have allowed a characterization of the statistical properties of the inhomogeneity.

This book focuses on developments over the last two decades in the areas of seismic wave propagation and scattering through the randomly heterogeneous structure of the earth with emphasis on the lithosphere. The characterization of the earth as a random medium is complementary to the classical stratified media characterization. We have tried to combine information from many sources to present a coherent introduction to the theory of scattering in acoustic and elastic materials that has been developed for the analysis of seismic data on various scales. Throughout the book, we include discussions of observational studies made using the various theoretical methods, so the reader can see the practical use of the methods for characterizing the earth. The audience includes both undergraduate and graduate students in the fields of physics, geophysics, planetary sciences, civil engineering, and earth resources. In addition, scientists and engineers who are interested in the structure of the earth and wave propagation characteristics are included.

Many people have helped us. Keiiti Aki's encouragement and pioneering work in this field were major factors in getting this project started. Yoichi Ando kindly invited us to contribute to this book series. We benefited from careful reviewing of the manuscript by Keiiti Aki and Ru-Shan Wu. We thank Masakazu Ohtake, Ryosuke Sato, Alexei Nikolaev, Tania Rautian, Vitaly Khalturin, and Eystein Husebye for continuous encouragement. Many of our colleagues, friends, and graduate students have collaborated with us in the development of stochastic studies of seismic wave scattering, helping us to learn more than we knew: Shigeo Kinoshita, Frank Scherbaum, Leigh House, Peter Roberts, Rafael Benites, Steve Hildebrand, W. Scott Phillips, Hans Hartse, Kazushige Obara, Mitsuyuki Hoshiba, Anshu Jin, Bernard Chouet, Alexander Gusev, Yuri Kopnichev, Osamu Nishizawa, Satoshi Matsumoto, Kiyoshi Yomogida, Teruo Yamashita, Yasuto Kuwahara, Kinichiro Kusunose, Yanis Baskoutas, Kazuo Yoshimoto, Hisashi Nakahara, Ken Sakurai, Kazutoshi Watanabe, Katsuhiko Shiomi, Lee Steck, Lian-Jie Huang, Takeshi Nishimura, Fred Moreno, and Tong Fei. Michael Fehler gratefully acknowledges James Albright and C. Wes Myers for encouraging his work on this book. Ruth Bigio assisted in drafting some of the figures. We thank Maria Taylor of Springer-Verlag/AIP Press for her encouragement throughout this project and Anthony Battle of Springer-Verlag for his cooperation.

*Haruo Sato
Michael C. Fehler*

Contents

1	Introduction	1
1.1	Scattering of Seismic Waves	1
1.2	Lithospheric Heterogeneity	6
1.3	Chapter Structure	9
1.4	Mathematical Symbols	10
1.5	Further Reading	11
2	Heterogeneity in the Lithosphere	13
2.1	Geological Evidence	13
2.2	Birch's Law	16
2.3	Random Inhomogeneity	18
2.3.1	Velocity Inhomogeneity Revealed from Well-Logs	18
2.3.2	Mathematical Description of Random Media	19
2.3.3	ACF of Velocity Inhomogeneity Revealed from Well-Logs and Rock Samples	27
2.4	Deterministic Imaging Using Seismological Methods	28
2.4.1	Refraction Surveys	29
2.4.2	Reflection Surveys	30
2.4.3	Receiver Function Method	34
2.4.4	Velocity Tomography	34
2.5	Scattering of High-Frequency Seismic Waves	40
2.5.1	Seismogram Envelopes	40
2.5.2	S-Coda Waves	42
2.5.3	Three-Component Seismogram Envelopes	49
2.5.4	Broadening of Seismogram Envelopes and Excitation of the Orthogonal-Component of Motion	50
2.5.5	Scattering of Ultrasonic Waves in Rock Samples	57
2.5.6	Cross-Correlation Function of Ambient Noise	59

3	Phenomenological Study of Coda Waves	63
3.1	Coda Excitation Models	65
3.1.1	Scattering Characteristics	65
3.1.2	Single Scattering Models	66
3.1.3	Diffusion Model	72
3.1.4	Energy-Flux Model	73
3.1.5	Simulations of Wave Scattering	75
3.2	Coda Analysis	78
3.2.1	Measurements of Total Scattering Coefficient	78
3.2.2	Measurements of Coda Attenuation	80
3.2.3	Duration Magnitude	84
3.2.4	Lg Coda	85
3.2.5	Coda Amplitude Decay for a Long Lapse-Time Range	86
3.2.6	Rayleigh-Wave Coda at Long Periods	88
3.3	Coda Normalization Method	92
3.3.1	Site Amplification Measurements	93
3.3.2	Source Radiation Measurements	97
3.3.3	Attenuation Measurements	99
3.4	Spatial Variation of Medium Heterogeneities	103
3.4.1	Spatial Variation of Scattering Characteristics	103
3.4.2	Spatial Variation of Intrinsic Absorption	105
3.4.3	Reflection from a Subducting Oceanic Slab	106
3.5	Temporal Change in Medium Characteristics	107
3.5.1	Temporal Change in Coda Attenuation and Scattering	108
3.5.2	Temporal Change in Velocity	114
3.5.3	Temporal Change in Site Factors	115
3.6	Related Seismogram Envelope Studies	117
3.6.1	Precursor and Coda Associated with Core Phase	117
3.6.2	Back Scattering of T-Waves by Seamounts	118
3.6.3	Envelope Correlation Method for Locating Low-Frequency Events	121
3.7	Further Reading	123
4	Born Approximation for Wave Scattering in Inhomogeneous Media	125
4.1	Scalar Waves	125
4.1.1	Born Approximation for a Localized Velocity Inhomogeneity	125
4.1.2	Scattering by Random Velocity Inhomogeneities	130
4.2	Elastic Vector Waves	135
4.2.1	Born Approximation for a Localized Elastic Inhomogeneity	135
4.2.2	Reduction of Independent Parameters by Using Birch's Law	141

4.2.3	Scattering by Random Elastic Inhomogeneities.....	145
4.2.4	Conversion Scattering Between Body and Rayleigh Waves	148
5	Attenuation of High-Frequency Seismic Waves	153
5.1	Measurements of Attenuation in the Lithosphere.....	153
5.2	Intrinsic Attenuation Mechanisms.....	154
5.3	Scattering Attenuation in Random Inhomogeneities	160
5.3.1	Travel-Time Corrected Born Approximation for Scalar Waves	162
5.3.2	Travel-Time Corrected Born Approximation for Vector Waves.....	169
5.3.3	Evaluation of Cutoff Scattering Angle	178
5.3.4	Diffraction Effects	179
5.4	Scattering Attenuation Due to Distributed Cracks and Cavities.....	180
5.5	Further Reading	184
6	Synthesis of Three-Component Seismogram Envelopes of a Small Earthquake	185
6.1	Earthquake Source	186
6.1.1	Point Shear-Dislocation Source	186
6.1.2	Omega-Square Model for the Source Spectrum	188
6.2	Envelope Synthesis in an Infinite Space.....	189
6.2.1	Geometry of Source and Receiver	189
6.2.2	Power Spectral Density of Velocity Wavefield	191
6.2.3	Numerical Simulations	198
6.3	Envelope Synthesis on the Free Surface of a Random Elastic Medium.....	202
6.3.1	Body-Wave Reflection at the Free Surface	203
6.3.2	Conversion Between Body Waves and Rayleigh Waves	208
6.4	Further Reading	210
7	Wave Propagation in Random Media and the Radiative Transfer Theory	211
7.1	Scalar Waves in Random Media	212
7.1.1	Scalar Wave Equation	212
7.1.2	Green’s Function for a Homogeneous Medium	213
7.1.3	Random Media.....	213
7.2	First Order Smoothing Method	214
7.2.1	Equation for the Mean Wave	214
7.2.2	Mass Operator	215
7.2.3	Mean Green’s Function.....	216
7.3	Radiative Transfer Equation	221
7.3.1	Multi-Scale Analysis	222
7.3.2	Radiative Transfer Equation and Scattering Coefficient	230

7.4	Radiative Transfer Equation in Integral Form	232
7.4.1	Scalar Wave Case	232
7.4.2	Elastic Wave Case	235
7.5	Diffusion Approximation	237
7.5.1	Scalar Wave Case	238
7.5.2	Elastic Wave Case	240
7.6	Further Reading	243
8	Envelope Synthesis Based on the Radiative Transfer Theory	245
8.1	Isotropic Scattering and Isotropic Source Radiation.....	246
8.1.1	One-Dimensional Case	246
8.1.2	Two-Dimensional Case	249
8.1.3	Three-Dimensional Case	251
8.1.4	Multiple Lapse Time Window Analysis (MLTWA).....	258
8.2	Isotropic Scattering with Conversion Between P- and S-Wave Modes.....	267
8.2.1	Seismogram Envelopes of Microearthquakes	267
8.2.2	Radiative Transfer Equation	268
8.2.3	Seismogram Envelopes from an Explosion Source in Volcano	275
8.3	Isotropic Scattering and Nonspherical Source Radiation.....	282
8.3.1	Radiative Transfer Equation	282
8.3.2	Envelopes for a Point Shear-Dislocation Source	288
8.3.3	Inversion for Energy Radiation from a Large Earthquake Fault.....	290
8.4	Nonisotropic Scattering and Isotropic Source Radiation	294
8.4.1	Radiative Transfer Equation	294
8.4.2	Simulation of Energy Density in Space and Time	299
8.5	Surface-Wave Envelopes on the Spherical Earth	303
8.5.1	Single Isotropic Scattering Model	303
8.5.2	Multiple Isotropic Scattering Model.....	308
8.5.3	Decay of Late Coda Envelope	309
8.6	Monte Carlo Simulation	309
8.6.1	Direct Simulation Monte Carlo Method	309
8.6.2	Study of Medium Heterogeneities by Using the Monte Carlo Simulation.....	312
8.7	Further Reading	317
9	Parabolic Equation and Envelope Synthesis Based on the Markov Approximation	319
9.1	Amplitude and Phase Distortions of Scalar Waves	320
9.1.1	Parabolic Equation in Random Media	320
9.1.2	Transverse Correlations of Amplitude and Phase Fluctuations	323
9.1.3	Measurements of Amplitude and Phase Fluctuations.....	328
9.1.4	Velocity Shift	331

- 9.2 Envelope Synthesis of Scalar Waves Based on the Markov Approximation 335
 - 9.2.1 Envelope of a Plane Wavelet 336
 - 9.2.2 Envelope of a Spherical Wavelet 347
 - 9.2.3 Monte Carlo Simulation of Envelope 356
 - 9.2.4 Comparison with FD Simulations in 2-D Random Media 362
 - 9.2.5 Using Markov Envelope in Radiative Transfer Theory 368
 - 9.2.6 Observation of Envelope Broadening 369
- 9.3 Envelope Synthesis of Vector Waves Based on the Markov Approximation 378
 - 9.3.1 Vector-Component Envelopes of a Plane P-Wavelet 380
 - 9.3.2 Vector-Component Envelopes of a Plane S-Wavelet 386
 - 9.3.3 Comparison with FD Simulations in 2-D Random Elastic Media 390
 - 9.3.4 Envelopes on the Free Surface 392
 - 9.3.5 Observation of Vector-Wave Envelopes 395
 - 9.3.6 Envelopes of a Spherical P-Wavelet 396
 - 9.3.7 Envelopes of a Spherical P-Wavelet in Nonisotropic Random Elastic Media 397
- 9.4 Further Reading 399
- 10 Green’s Function Retrieval from the Cross-Correlation Function of Random Waves 401**
 - 10.1 Green’s Function Retrieval for a Homogeneous Medium 402
 - 10.1.1 Scalar Waves 402
 - 10.1.2 Elastic Waves 418
 - 10.1.3 White-Spectrum Random Waves in a Bounded Medium 425
 - 10.2 Green’s Function Retrieval for a Scattering Medium 429
 - 10.2.1 Green’s Function for a Scattering Medium 429
 - 10.2.2 Illumination by Noise Sources Distributed on a Large Spherical Shell 433
 - 10.2.3 Illumination by Uniformly Distributed Noise Sources 437
 - 10.2.4 Green’s Function Retrieval from the CCF of Singly-Scattered Coda Waves 440
 - 10.3 Analyses of CCF of Ambient Noise 443
 - 10.3.1 Velocity Analysis and Application to Tomography 444
 - 10.3.2 Monitoring the Temporal Change in the Crustal Medium Property 446
 - 10.4 Further Reading 450

11 Epilogue	451
11.1 Developments of Measurement Capability	451
11.2 Developments in Theory and New Methods	452
11.3 Developments in Observations	453
11.4 Necessary Developments in Future	454
A Spherical Harmonic Functions and Wigner 3-j Symbols	457
References	461
Index	489

Chapter 1

Introduction

1.1 Scattering of Seismic Waves

The region of the earth down to about 100 km is called the lithosphere. Rigorously speaking, lithosphere refers to the solid portion of the earth that overlays the low velocity zone or the asthenosphere, and the thickness varies from place to place depending on the tectonic setting; however, we will use this term loosely for the upper 100 km of the earth that consists of the crust and the uppermost mantle. The structure of the earth's crust has been investigated using layered models since the discovery of the Mohorovicic discontinuity or Moho at the base of the crust (Mohorovičić 1909) and the Conrad discontinuity in the mid crust (Conrad 1925). The characterization of the earth as a random medium is complementary to the classical stratified medium characterization. Well-log data collected in the shallow crust exhibit strong random heterogeneity with short wavelengths (e.g. Holliger 1996; Shiomi et al. 1997; Wu et al. 1994). Surveys using the reflection method, such as those conducted by the Consortium for Continental Reflection Profiling (COCORP) reveal that the Moho is not a simple discontinuity but a transition zone consisting of many segments of small reflectors, and that the crust is heterogeneous on scales of a few kilometers to tens of kilometers (Schilt et al. 1979). Moreover, the development of regional velocity tomography (e.g. Aki and Lee 1976; Aki et al. 1976; Zhang and Thurber 2003; Zhao et al. 2009), which uses travel-time readings from seismograms of teleseismic waves, local earthquakes, or man-made sources such as explosions, has allowed the delineation of the inhomogeneous velocity structure on scales from a few meters to a few tens of kilometers in many regions of the world.

As an example, we show short-period velocity seismograms (transverse horizontal component) of an M_W 4.8 earthquake in Fig. 1.1b, where all the traces are shown in the same gain. Figure 1.1c is a magnification of 200 times. The earthquake epicenter and stations used are shown in Fig. 1.1a. The maximum amplitude decreases as epicentral distance increases; however, the amplitude of the tail portion smoothly decays with increasing lapse time and their amplitudes are nearly equal

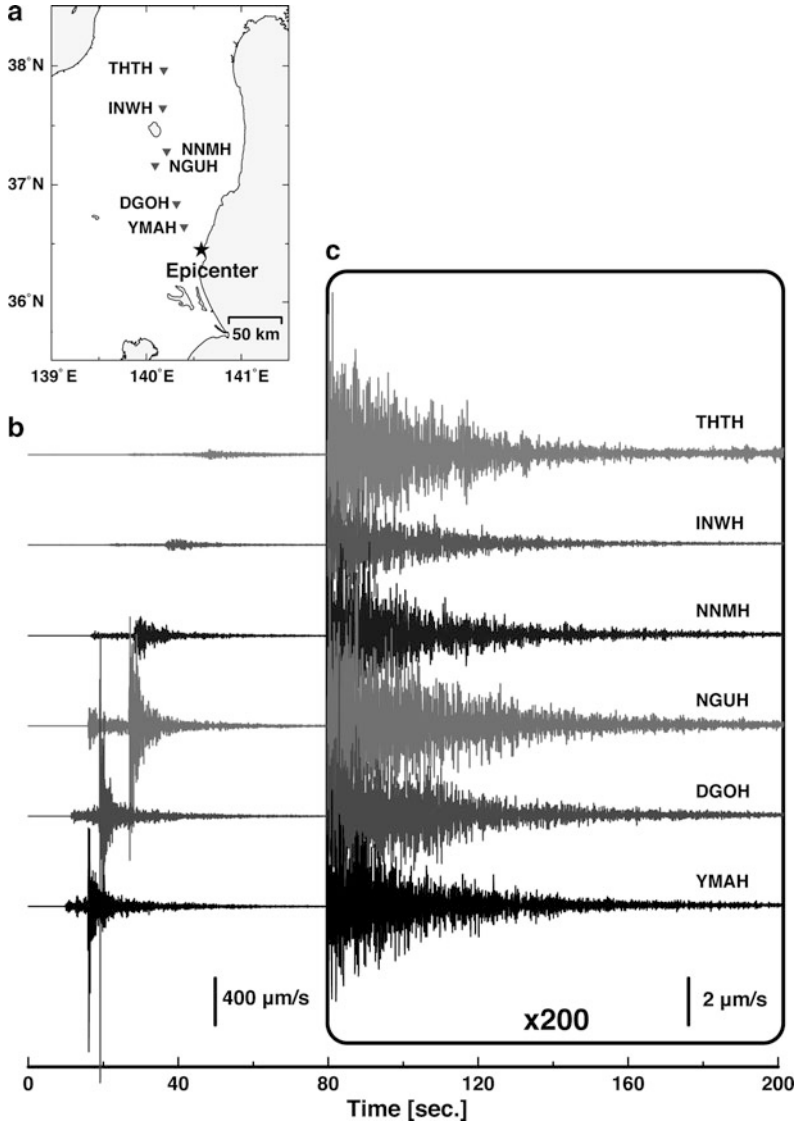


Fig. 1.1 (a) Epicenter (star) of an M_W 4.8 earthquake with 55.3 km in focal depth and Hi-net stations (reversed triangles) of NIED in Honshu, Japan. (b) Velocity seismograms (horizontal transverse component) arranged from bottom to top by increasing epicentral distance, where the gain is the same for all the traces. (c) Magnification of 200 times

each other independent of epicentral distance at large lapse times. [Aki \(1969\)](#) first focused interest on the appearance of continuous wave trains in the tail portion of individual seismograms of local earthquakes as direct evidence of the random heterogeneity of the lithosphere. These wave trains, which Aki named “coda,” look

like random signals having an envelope whose amplitude smoothly decreases with increasing lapse time measured from the origin time of an earthquake. Aki proposed that coda is composed of incoherent waves scattered by distributed heterogeneities in the lithosphere. [Rautian and Khalturin \(1978\)](#) observed that coda envelopes of a local earthquake decay stably irrespective of epicentral distance and coda envelopes at all distances have a similar lapse time dependence. Those observed characteristics of seismic coda are strongly linked to the historic and continuing use of the duration of a recorded seismogram as a measure of the magnitude of a local earthquake ([Solov'ev 1965](#); [Tsumura 1967](#)).

Historically, most seismograms of local and regional earthquakes, those recorded at distances to as long as 300 km, were recorded on regional networks whose primary function was to record first arrival times to be used for locating earthquakes. Since these networks relied on analog transmission of data from multiple stations over radio link or phone lines, the dynamic range of the recordings was limited. This necessitated that the stations be run at high gain to allow identification of the first arriving P-waves from small local earthquakes. High gains often clipped the early portions of seismograms. The first methods for analysis of coda waves were thus developed to be used on seismograms whose early portions were clipped, particularly for larger earthquakes. Coda analysis gained in popularity as a means for obtaining information about seismic sources and medium properties from data collected by these high-gain and small dynamic range networks.

Later, coda waves were thought to offer a useful seismological tool for the quantitative estimation of the strength of random heterogeneity ([Aki and Chouet 1975](#); [Sato 1978](#)). As seismometers were placed in boreholes where ambient seismic noise was greatly reduced compared to that on the ground surface and as the onset of digital seismic network allowed dynamic range to be increased, envelopes of entire seismograms including both the maximum amplitude portion and the coda portion were recorded and modeled to learn more about the random heterogeneity of the earth's lithosphere by using frequencies in the range of 1–30 Hz.

Models for seismic wave propagation through inhomogeneous elastic media have been developed using deterministic approaches such as mode theory for layered structures or high-frequency approaches such as the eikonal approximation. However, array analysis has shown that coda waves are not regular plane waves coming from the epicenter, but are composed of scattered waves coming from all directions ([Aki and Tsujiura 1959](#)). Ray theoretical approaches are thus generally unsuitable for the study of coda. In the 1970s, S-coda waves were studied by using the single scattering approximation to the wave equation as one end-member model and a model based on the diffusion equation as another end-member (e.g. [Aki and Chouet 1975](#); [Kopnichev 1975](#); [Sato 1977a](#); [Wesley 1965](#)). The single scattering theory based on the Born approximation for elastic media has been used to explain characteristics of observed three-component seismogram envelopes for a point shear-dislocation earthquake source ([Sato 1984a](#)). In parallel with the development of theoretical modeling, parameters phenomenologically characterizing S-coda such as total scattering coefficient g_0 and S-coda attenuation Q_c^{-1} have been measured in many regions and compared with seismotectonic settings. Total scattering

coefficient g_0 is a measure of scattering power per unit volume. S-coda attenuation Q_c^{-1} is a parameter describing the exponential decay rate of Scoda envelope with increasing lapse time after the correction for geometrical decay. There have been reports of temporal changes in these parameters in relation to the occurrence of large earthquakes (e.g. [Gusev and Lemzikov 1985](#); [Jin and Aki 1986](#)).

As a natural consequence of energy conservation, the excitation of coda waves in scattering media means that the direct wave loses energy with increasing propagation distance. Until the 1970s, however, there was little theoretical understanding of the contribution of scattering loss as a mechanism for the attenuation of seismic wave amplitude with travel distance. Intrinsic absorption was considered dominant and frequency-independent. By using data from dense regional seismic networks that were constructed in U.S.A. and Japan for observation of microearthquakes, the frequency dependence of S-wave attenuation Q_S^{-1} was measured. As we will discuss in Chap. 5, Q_S^{-1} decreases with increasing frequency for frequencies higher than 1 Hz. Combining attenuation measurement for lower frequencies made on surface waves, [Aki \(1980a\)](#) conjectured that Q_S^{-1} has a peak frequency around 0.5 Hz. If scattering is the dominant mechanism of attenuation, the observed frequency dependence cannot be explained by the ordinary stochastic mean field theory for wave propagation through random media, which predicts that scattering attenuation increases with frequency. To resolve the discrepancy, improvements were introduced to the stochastic theory to make it a more realistic model for the practical seismological measurement of amplitude attenuation. One improvement was to calculate the scattering loss by integrating the energy of scattered waves only for scattering angles larger than 90° ([Wu 1982b](#)), and the other is to subtract the travel-time fluctuation caused by the slowly varying velocity fluctuation before using the stochastic averaging procedure in the mean field theory ([Sato 1982a](#)). Those models theoretically lead to scattering Q^{-1} having a peak and decreasing with frequency on both sides. The spectral structure of the random inhomogeneity has been studied by using those models and the observed frequency dependence of Q_S^{-1} .

The radiative transfer theory, where the phase information is ignored, is useful for explaining high-frequency coda envelopes for radiation from a point source in a scattering medium. This theory has been extended to include phenomena of importance to propagation in the earth such as impulsive radiation, nonisotropic scattering and nonspherical radiation from a point shear-dislocation earthquake source (e.g. [Sato 1994a](#); [Shang and Gao 1988](#); [Wu and Aki 1988](#); [Zeng et al. 1991](#)). In parallel, Monte Carlo simulations have been developed for numerical syntheses of seismogram envelopes on the basis of the radiative transfer theory in more complex structures (e.g. [Gusev and Abubakirov 1987](#); [Hoshiya 1994](#); [Sens-Schönfelder et al. 2009](#); [Yoshimoto 2000](#)). The radiative transfer theory with conversion scattering between P- and S-wave modes was effectively used to analyze seismograms of artificial explosions in strongly heterogeneous regions beneath volcanoes ([Yamamoto and Sato 2010](#)). As the concept of scattering loss was accepted in the seismological community, [Wu \(1985\)](#) introduced the seismic albedo as a phenomenological measure of the contribution of scattering attenuation to the total attenuation. [Fehler et al. \(1992\)](#) proposed a method known as the

multiple lapse-time window analysis to estimate the seismic albedo by the analysis of complete S-seismogram envelopes. The method uses solutions of the radiative transfer theory for the multiple isotropic scattering process for spherical radiation from a point source (Hoshiya et al. 1991; Zeng et al. 1991). There have been many regional measurements of scattering and intrinsic attenuation made using this method (e.g. Carcolé and Sato 2010; Mayeda et al. 1992).

Although the source duration of small local earthquakes is often less than 1 s, the apparent duration of S-wave envelopes is found to be much longer than 1 s at hypocentral distances greater than 100 km (Sato 1989). Figure 1.2 shows horizontal transverse component seismograms (2–32 Hz) of an M_W 3.8 earthquake arranged by increasing epicentral distance as an example. Different from Fig. 1.1, each trace is normalized by its maximum amplitude. When we focus on the wave envelope from the S-onset to the time of the half maximum amplitude, we find that the apparent duration time of S-seismogram increases with increasing travel distance. At distances larger than 100 km, it becomes more than several seconds being much

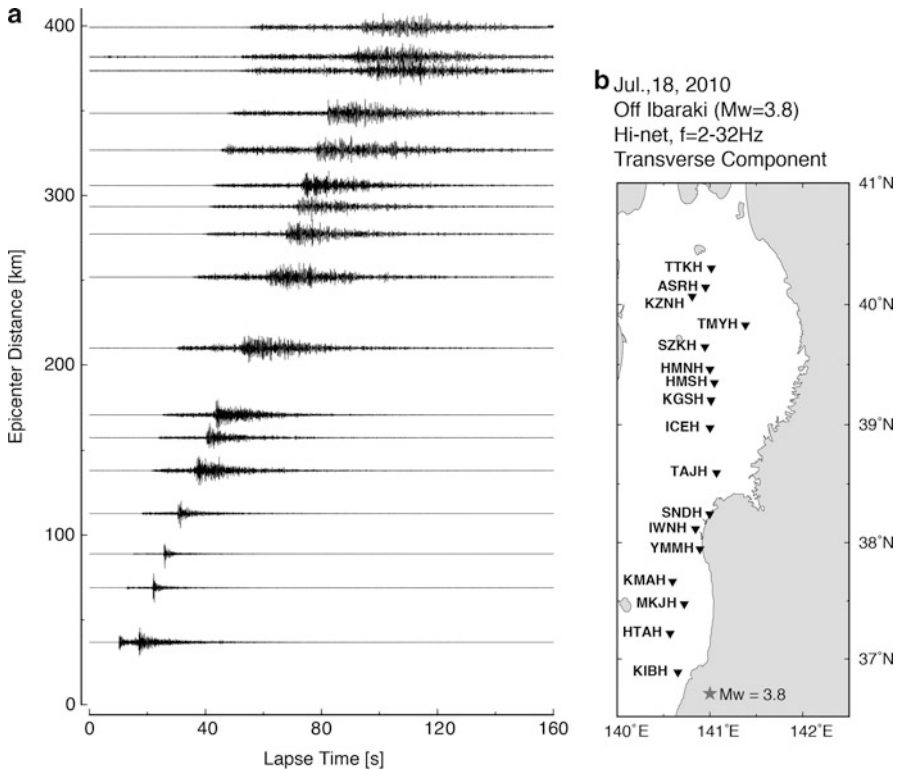


Fig. 1.2 (a) Envelope broadening of velocity seismograms (horizontal transverse component, 2–32 Hz) of an M_W 3.8 earthquake with increasing epicentral distance in northeastern Honshu, Japan, where each trace is normalized by its maximum amplitude. (b) Star and inverted triangles in the map are the epicenter and Hi-net stations of NIED, respectively

larger than the source duration estimated from the earthquake magnitude. We also see a delay of the envelope peak arrival from the S-onset. Each seismogram looks like a spindle without clear S-phase for distances larger than 200 km. Both the envelope broadening and the delay of the peak arrival were quantitatively studied by using the stochastic averaging method for the parabolic approximation to the wave equation, the Markov approximation, which was originally developed for optical waves or acoustic waves through media with randomly varying refractive index when the wavelength is smaller than the scale of the random inhomogeneities. The theory gives a good explanation of the effects of strong diffraction on the observed characteristics of the early portion of S-wave envelopes at large travel distances. The frequency dependence of envelope broadening with travel distance is controlled by the power spectrum of the random velocity inhomogeneities (Saito et al. 2002; Sato 1989). The envelope broadening was found to be stronger in the back-arc side of the volcanic front of the northern Japan compared with that in the fore-arc side, where the Pacific plate is subducting beneath the Japan arc (Obara and Sato 1995). Shearer and Earle (2004) estimated the velocity inhomogeneity in the mantle from the analysis of teleseismic P-wave envelopes using the envelope synthesis based on the radiative transfer theory combined with the Born approximation. Kubanza et al. (2007) put a focus on the excitation of the transverse component of teleseismic P-waves. They estimated the lithospheric heterogeneities from the energy partition into the transverse component by using the Markov approximation for vector-wave envelopes in random elastic media (Sato 2006).

The Green's function retrieval from the cross-correlation function of ambient noise has recently gained significant attention as a method to provide information about the structure of the earth. This method does not need any real natural earthquake sources nor artificial sources. First, the method was used to find the Rayleigh wave velocity (Campillo and Paul 2003), then it became possible to measure body wave velocity as well (Roux et al. 2005b). Monitoring the cross-correlation function (CCF) of ambient noise is useful also for detecting temporal changes in seismic velocity associated with earthquake activities (e.g. Brenguier et al. 2008). There have been attempts to measure the temporal change in the coda portion of the auto-correlation function of ambient noise, which might reflect a change in crustal heterogeneity (e.g. Maeda et al. 2010; Wegler and Sens-Schönfelder 2007). The retrieval of Green's function having a coda tail from the CCFs of random waves is possible even in a heterogeneous medium (e.g. Margerin and Sato 2011a; Sato 2009a, 2010; Snieder and Fleury 2010).

1.2 Lithospheric Heterogeneity

The excitation of S-coda is well quantified by the total scattering coefficient of S-waves g_0 , which is the reciprocal of the mean free path. Measurements of g_0 -value in the lithosphere have often been made based on the radiative transfer theory

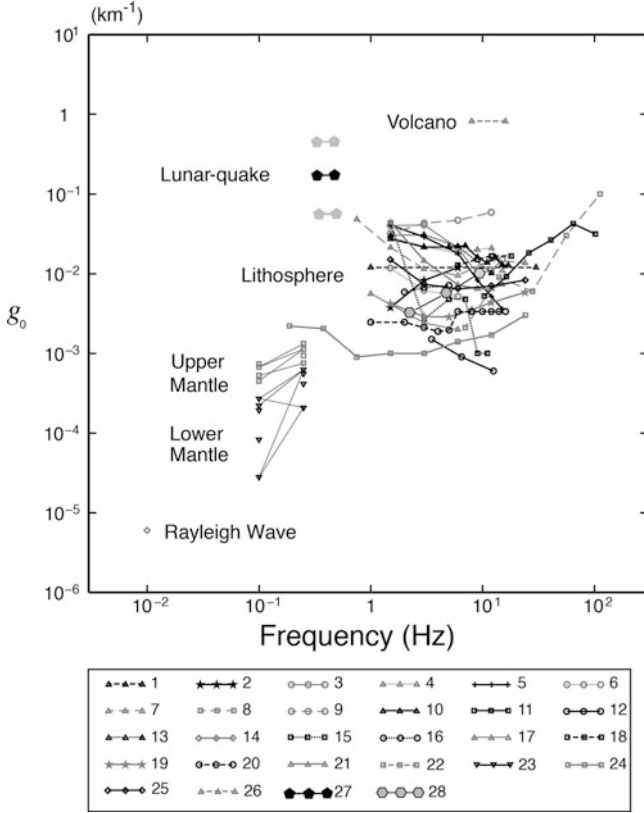


Fig. 1.3 Regional measurements of the total scattering coefficient of S-waves [Courtesy of K. Emoto]: 1 Kanto, Japan (Sato 1978), 2 Kanto-Tokai, Japan (Fehler et al. 1992), 3 Long Valley, California, 4 Central California, 5 Hawaii (Mayeda et al. 1992), 6 Average in Japan (Hoshiya 1993), 7 Southern California (Jin et al. 1994), 8 Southern California, (Leary and Abercrombie 1994), 9 Northern Greece (Hatzidimitriou 1994), 10 Southern Spain ($\Delta = 0 - 170$ km) (Akinci et al. 1995), 11 Southern California (Adams and Abercrombie 1998), 12 Northeastern Venezuela (Ugalde et al. 1998), 13 Eastern Turkey (Akinci and Eyidogan 2000), 14 Rayleigh waves in long periods (Sato and Nohechi 2001), 15 Southern Apennines, Italy (Bianco et al. 2002), 16 Central France (Lacombe et al. 2003), 17 South Central Alaska (Dutta et al. 2004), 18 Southern Netherlands (Goutbeek et al. 2004), 19 Northeastern Colombia (Vargas et al. 2004), 20 Northeastern Italy (Bianco et al. 2005), 21 Southern Sicily, Italy (Giampiccolo et al. 2006), 22 Lithosphere and Upper Mantle (0 – 670 km) (Lee et al. 2003, 2006), 23 Lower Mantle (>670 km) (Lee et al. 2003, 2006), 24 Germany (Sens-Schönfelder and Wegler 2006), 25 Average in Japan (Carcolé and Sato 2010), 26 Asama volcano, Japan (Yamamoto and Sato 2010), 27 Lunar quakes (Dainty and Toksöz 1981), 28 Transport scattering coefficient g_m in Norwegian crust (Przybilla et al. 2009)

from octave-width frequency band S-wave envelopes. Figure 1.3 summarizes recent regional measurements of g_0 -value against frequency. Most of the measurements are based on the isotropic scattering model; however, some are measurements of backscattering coefficient g_π in the single scattering regime or the transport

scattering coefficient g_m , which is the effective isotropic scattering coefficient in the multiple scattering regime of nonisotropic scattering process as will be discussed in Chap. 7.

Reported g_0 values in the lithosphere are distributed from 10^{-3} km^{-1} to $5 \times 10^{-2} \text{ km}^{-1}$ around 10^{-2} km^{-1} for the frequency range of 1 – 30 Hz. A large value of $g_0 \approx 1 \text{ km}^{-1}$ was found from the analysis of artificial explosions on an active volcano (Yamamoto and Sato 2010). From the analysis of lunar quakes by using the diffusion model, the g_0 -value estimated ranges from 0.05 to 0.5 km^{-1} (Dainty and Toksöz 1981). Lee et al. (2003, 2006) analyzed coda envelopes of regional earthquakes before and after the ScS arrival around 900 s in lapse time from the origin time using the numerically simulated envelopes based on the multiple isotropic scattering model with the PREM model for velocity and total attenuation. They reported lower g_0 -values in the 4 s and 10 s period bands in the upper mantle compared with those in the lithosphere. The g_0 -value becomes much smaller in the lower mantle. For comparison, the g_0 -value of long-period Rayleigh waves propagating completely around the earth is of the order of 10^{-6} km^{-1} , which is much smaller than those of S-waves in short periods in the lithosphere (Sato and Nohechi 2001).

On the basis of the stochastic wave theory for random media, there have been measurements of the power spectral density function (PSDF) $P(m)$ of the fractional velocity fluctuation $\delta V(\mathbf{x})/V_0$. Figure 1.4 summarizes recent measurements of the

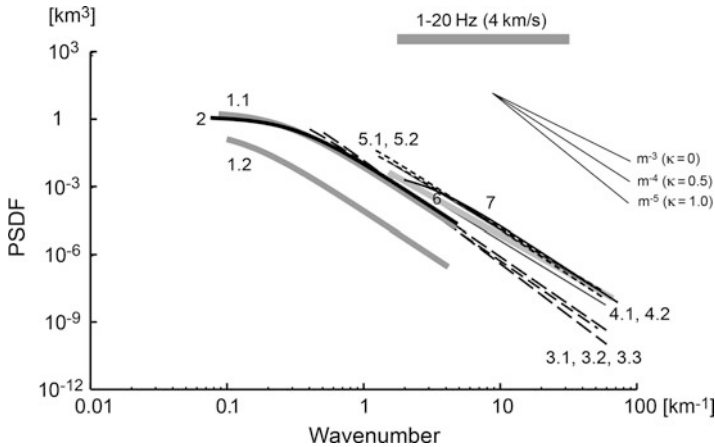


Fig. 1.4 Measurements of the PSDF of the fractional velocity fluctuation in the lithosphere and mantle: *Teleseismic P-wave envelopes*: 1.1 Upper mantle, 1.2 Lower mantle (0.5 – 2.5 Hz) (Shearer and Earle 2004), 2 Baltic Shield (0.5 – 5 Hz) (Hock et al. 2000). *S-wave envelopes*: 3.1, 3.2, 3.3 Fore-arc, Japan (2 – 16 Hz) (Saito et al. 2002, 2005; Takahashi et al. 2009), 4.1, 4.2 Kurikoma and Iwate volcanoes (2 – 16 Hz, 20 – 60 km in depth), NE Japan (Takahashi et al. 2009), 5.1, 5.2 Scattering loss and S-coda excitation (1 – 30 Hz) (Sato 1984a, 1990), 6 Crust, Norway (2 – 10 Hz) (Przybilla et al. 2009). *P- and S-wave envelopes*: 7 Upper crust, Nikko, Japan (8 – 16 Hz) (Yoshimoto et al. 1997b). Gray bar shows the corresponding frequency range for 4 km/s velocity

PSDF in km^3 in the lithosphere and mantle against wavenumber m in km^{-1} . From the frequency-dependence analysis of P-wave envelope broadening of teleseismic events using the radiative transfer theory with Born scattering coefficients, the PSDF in the lower mantle (line 1.2 in Fig. 1.4) was found to be smaller than that in the lithosphere and upper mantle (line 1.1). PSDFs were intensively measured in northern Japan, where the Pacific plate is subducting beneath the Japan arc, from the frequency-dependence analysis of envelope broadening of S-wave seismograms of small local earthquakes by using the Markov approximation. The PSDFs beneath Quaternary volcanoes (lines 4.1 and 4.2) are larger and their decay rates with increasing wavenumber are smaller than those in the fore-arc side (east side) of the volcanic front (lines 3.1, 3.2, 3.3). Lines 5.1 and 5.2 show PSDFs revealed from S-wave scattering loss and coda excitation analysis of microearthquake seismograms in the lithosphere. Line 6 is measured from S-envelopes of crustal earthquakes in Norway, and line 7 is measured from P- and S-coda excitation in the upper crust in Nikko, Japan by using the radiative transfer theory with Born scattering coefficients.

1.3 Chapter Structure

This book focuses on developments over the last four decades in the areas of seismic wave propagation and scattering through the randomly inhomogeneous earth structure, especially in the lithosphere. This book introduces both observed scattering phenomena of short-period seismic waves and mathematical tools for the description of medium heterogeneity and wave propagation and scattering in random media.

In Chap. 2, we will briefly review typical measurements and observations that support that the lithosphere can be viewed as being randomly heterogeneous. We also introduce basic mathematics to describe random inhomogeneities. Chapter 3 introduces a phenomenological description of coda-wave excitation, which forms the basis of S-coda analysis and the coda-normalization method. Various aspects of scattering phenomena are also discussed.

Chapter 4 provides the Born approximation for scattering in inhomogeneous elastic media. Scalar wave theory is presented to introduce the mathematics. In Chap. 5, we will first review the frequency dependence of observed attenuation and discuss several proposed mechanisms of intrinsic absorption. Then we will introduce an improved stochastic averaging method that is consistent with observational methods. This method describes the frequency dependence of scattering attenuation in random media. In Chap. 6, we will develop a method for synthesizing three-component seismogram envelopes of a local earthquake based on the summation of the powers of waves that have been singly scattered by random elastic inhomogeneities. This model includes the effects of nonspherical radiation from a point shear-dislocation source in addition to nonisotropic scattering from the inhomogeneities.

Chapter 7 provides the first-order smoothing method to derive the dispersion relation of the mean wave in random media, and a statistical derivation of the radiative transfer equation by using the multi-scaling analysis. The diffusion equation is derived from the radiative transfer theory. In Chap. 8, we will discuss the synthesis of seismogram envelopes based on the radiative transfer theory for the case of spherical source radiation and multiple isotropic scattering. After the theory is developed, we will present the multiple lapse-time window analysis for the estimation of seismic albedo. We will also describe extensions of the theory to cases of non-spherical source radiation, nonisotropic scattering, and conversion scattering between P- and S-wave modes.

In Chap. 9, we will review the parabolic approximation for scalar waves in random media and its stochastic treatment. Then we will provide the Markov approximation for the synthesis of scalar and vector wave envelopes in random media. This approximation well explains observed envelope broadening.

Chapter 10 introduces the theory for the Green's function retrieval from the CCF of random waves. Several examples of its applications to data are provided.

In Chap. 11, we summarize the state of the art and discuss possible future developments.

1.4 Mathematical Symbols

Mathematical symbols are not completely systematic in this book and they are defined in each chapter; however, there are some common rules. Here we summarize those rules and symbols and accents as follows. We use the Einstein summation convention for the summation of vector components as $\mathbf{ab} = a_j b_j = \sum_{j=1}^3 a_j b_j$, where bold symbols mean vectors. We often use representations (a_1, a_2, a_3) for Cartesian vector components (a_x, a_y, a_z) and (x_1, x_2, x_3) for (x, y, z) . An overdot $\dot{}$ means the derivative taken with respect to time. Symbol $d\mathbf{x} = dx dy dz$ means a volume element in Cartesian coordinates and $d\mathbf{x} = r^2 dr d\Omega(\theta, \varphi)$ in spherical coordinates, where $d\Omega(\theta, \varphi) = \sin \theta d\theta d\varphi$ is a solid angle element. We define the Fourier decomposition of function $f(\mathbf{x}, t)$ in space and time using a plane wave element $\exp(i\mathbf{kx} - i\omega t)$ as

$$\begin{aligned}
 f(\mathbf{x}, t) &= \frac{1}{2\pi} \int_{-\infty}^{\infty} \hat{f}(\mathbf{x}, \omega) e^{-i\omega t} d\omega \\
 &= \frac{1}{(2\pi)^3} \iiint_{-\infty}^{\infty} \tilde{f}(\mathbf{k}, t) e^{i\mathbf{kx}} d\mathbf{k} \\
 &= \frac{1}{(2\pi)^4} \iiint \int_{-\infty}^{\infty} \hat{\tilde{f}}(\mathbf{k}, \omega) e^{i\mathbf{kx} - i\omega t} d\mathbf{k} d\omega, \quad (1.1)
 \end{aligned}$$

where a tilde \sim and a hat $\hat{}$ mean the Fourier transform with respect to space coordinate and time, respectively. We note that a hat is also used for the Laplace transform with respect to time, which is discriminated by argument s , when we solve the radiative transfer theory in Chaps. 7 and 8:

$$\hat{f}(s) = \int_0^{\infty} f(t) e^{-st} dt. \quad (1.2)$$

A round cap \sim means the spectral density. An over-bar $\bar{}$ means the normalized non-dimensional quantity. A breve $\breve{}$ means the Fourier transform with respect to the transverse coordinate. Symbols Δ and Δ_{\perp} mean Laplacian and Laplacian in the transverse plane, respectively. Angular brackets $\langle \dots \rangle$ mean the average over the ensemble of random media in most chapters; however, the angular brackets mean the average over the ensemble of noise source distributions in Chap. 10. Angular brackets with subscript T $\langle \dots \rangle_T$ means the average over time. We note that italic font “ G ” and sanserif font “ \mathbf{G} ” are used for the Green’s function of waves and that of energy density, respectively.

1.5 Further Reading

Following books and monographs treat the subjects discussed in this book. [Chandrasekhar \(1960\)](#) is a classic textbook for radiative transfer theory. [Ishimaru \(1978\)](#) and [Rytov et al. \(1989\)](#) offer advanced mathematical tools for the study of wave propagation in random media. [Shapiro and Hubral \(1999\)](#) focuses on wave propagation through stratified random media. [Goff and Holliger \(2003\)](#) summarizes the observed crustal heterogeneity. [Apresyan and Kravtsov \(1996\)](#) introduces mathematical relations between the wave theory in random media and the radiative transfer theory. There are two reports of the IASPEI task group on “Scattering and Heterogeneity”: [Wu and Maupin \(2007\)](#) compiles mathematical modeling of wave propagation in inhomogeneous media, and [Sato and Fehler \(2008\)](#) compiles the recent developments in studies on seismic wave scattering and earth medium heterogeneities. There are several special issues of journals which focus on these subjects (e.g. [Husebye 1981](#); [Korn et al. 1997](#); [Sato 1991b](#); [Wu and Aki 1988b, 1989, 1990](#)).

Chapter 2

Heterogeneity in the Lithosphere

Geologists and geophysicists have numerous ways to investigate and characterize heterogeneity in the earth. Geophysical characterization includes measurement of physical properties such as seismic velocities and density of rocks. Geological characterization includes mineralogical composition and grain size distribution that are both controlled by the processes by which the rock evolved. Geologists observe the surface of the earth and analyze rocks that originated from within the earth for signs of heterogeneity. The wide variation of rocks erupted from volcanoes provides geochemical and geological evidence of heterogeneity within the earth. Tectonic processes such as folding, faulting, and large scale crustal movements associated with plate tectonics contribute to making the lithosphere heterogeneous. Rocks recovered from boreholes show wide variation and rapid changes in chemical composition with depth. Geophysical measurements in wells show correlation and lack of correlation with chemical composition of the rocks, indicating that mineral composition alone is not the only factor that controls the physical properties of rocks. Deterministic seismic studies reveal a wide spatial variation in elastic properties within the earth's lithosphere. Scattering of high-frequency seismic waves reveals the existence of small scale heterogeneities in the lithosphere.

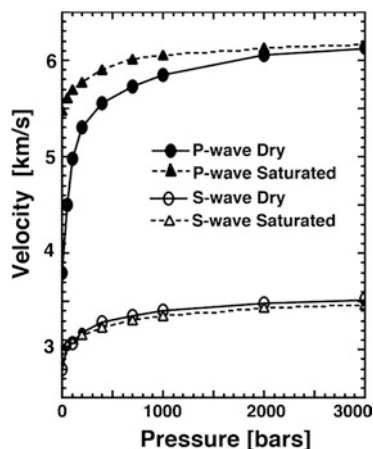
In this chapter, we will give an overview of various types of observations to show and methods to evaluate the heterogeneous structure of the earth's lithosphere. We will also introduce basic mathematical methods to characterize the random fluctuation of medium properties.

2.1 Geological Evidence

The earth's crust contains a wide variation of rock types. Table 2.1 lists the P-wave velocity α and S-wave velocity β of some common rocks that compose the earth's crust. Seismic velocities are different for different rock types. The earth has heterogeneities on many scales. Rocks have crystals that range in size from

Table 2.1 Velocities of rocks in the earth's crust. (Data for near-surface rocks from [Press 1966](#))

Rock type	Location	P-wave Vel. α	S-Wave Vel. β
Granite	Westerly, Rhode Is., U.S.A.	5.76 km/s	3.23 km/s
Quartz Monzonite	Westerly, Rhode Is., U.S.A.	5.26	2.89
Andesite	Colorado, U.S.A.	5.23	2.73
Basalt	Germany	5.0–6.4	2.7–3.2
Limestone	Argillaceous, Texas, U.S.A	5.71–6.03	3.04–3.04
Slate	Everett, Mass., U.S.A.	4.27	2.86

Fig. 2.1 Laboratory measurements of the variation of wave velocity in dry and water saturated Westerly granite. (Data from [Nur and Simmons 1969](#), copyright by Elsevier)

fractions of mm to a few cm in scale. Properties of minerals that make up rocks in the earth's crust vary a great deal ([Simmons and Wang 1971](#)). For example, the bulk modulus of quartz, one of the major constituents of crustal rocks, is about 0.39×10^{12} dyn/cm² whereas that of the mineral plagioclase, another major constituent, is about 0.65×10^{12} dyn/cm² ([Simmons and Wang 1971](#)). Thus, the relative abundance of these two minerals in a rock can greatly influence its elastic properties.

In addition to mineralogy, fractures influence the elastic properties of a rock ([Simmons and Nur 1968](#)). Fractures range in size from submicroscopic to many tens of meters. Since fractures are more compliant than intact minerals, the spatial variations in fracture content and size can have a larger influence on elastic properties of crustal rocks than mineral composition. Figure 2.1 shows laboratory measurements of velocity variation with pressure for granite from Westerly, Rhode Island, U.S.A. The variation with pressure is due to the closure of fractures having lengths ranging from 0.01 mm to 1 cm and is typical of most crustal rocks. The P-wave velocity is more sensitive to the presence of fluids in the fractures than the S-wave velocity since fluids transmit compressional waves but not shear waves.

Anisotropy of rock properties can be significant and may vary with location, which increases rock heterogeneity. The presence of fractures can lead to anisotropy

of the elastic properties of the bulk rock. Fractures may have a preferential alignment that results from the way they were formed or due to the variation in stress magnitude as a function of orientation that causes some cracks to be open and some to be closed. Another type of anisotropy is a result of a layering of rocks, such as is present in many sedimentary formations. Tectonic processes may rotate the layering so that the preferential orientation of fast and slow directions of anisotropic media are not aligned with horizontal and vertical directions. A general overview of anisotropy can be found in [Helbig and Thomsen \(2005\)](#) and [Tsvankin et al. \(2010\)](#).

Intrusions of magma into preexisting country rock can result in dikes and sills that have different composition from the country rock. These dikes and sills can be as small as a few mm wide resulting in a rapid spatial variation in rock properties. Variations in rock properties in volcanic regions can occur on scales of a few m to a few km due to variations in composition of magmas erupted at differing stages of a volcano's life. The variation in tectonic provinces occurs over tens to hundreds of km. For example, the Cascade range in the western U.S.A. is largely made up of young volcanic rocks whose elastic properties are dramatically different from those of the old Precambrian rocks of the central U.S.A.

The earth's crust has largely been formed through magmatic processes. Large silicic batholiths like the Sierra Nevada, U.S.A. are the intrusive remains of volcanic complexes that have been eroded away. Geochemists argue that silicic rocks that intrude into the shallow crust and erupt at volcanoes were formed by either fractionation of iron-rich rocks that intrude into the lower crust from the mantle or by the transfer of heat from intruded iron-rich mantle rocks to silicic rocks in the deep crust ([Perry et al. 1990](#)). In either case, there will be high-velocity material remaining within the silicic crust. The velocity of the high-density material may be as high as 7.5 km/s ([Fountain and Christensen 1989](#)). If heat is transferred from mantle-derived magmas, the resulting magmas may have velocities of about 7.0 km/s. The intrusion process thus results in considerable heterogeneity in the earth's crust.

Characterization of heterogeneity in sedimentary rocks receives considerable attention because these rocks contain a majority of the world's hydrocarbons. Heterogeneity in sedimentary formations has many causes including changes in the source rocks from which the sediments were formed, variations in the cementing rocks together, variations in porosity and pore fluids, and the tectonic processes that act on the rocks after deposition. The deterministic heterogeneity in many sedimentary rocks is well characterized by the extensive amount of seismic imaging of various types, borehole logging, and geological characterization that has been conducted during the exploration for and development of hydrocarbon resources.

Other geological processes that contribute to heterogeneity in the lithosphere include erosion and metamorphism that act to transport rocks or change their character in place. Tectonic processes, such as faulting and folding, move rocks relative to one another and result in heterogeneity. Large scale movements of lithospheric plates distribute rocks having a common origin over a wide range. The collision of tectonic plates at plate boundaries, such as subduction zones or collision zones, causes rocks of differing types to come into contact.

2.2 Birch's Law

There are good correlation among P and S-wave velocities and mass density. From experimental data on rocks of many types, Birch (1960, 1961) found that seismic velocity increases roughly linearly with mass density for rocks having the same mean atomic weight, which is the atomic weight of the minerals that comprise the rocks averaged in proportion to the mass they contribute to the rock. Mean atomic weight for most crustal rocks ranges from about 21 for silica-rich rocks like granite to 22 for iron-rich igneous rocks. Figures 2.2a and b show P- and S-wave velocities in km/s measured at 10 kbar (1 GPa) pressure on common lithospheric rocks having mean atomic weights between 20.5 and 22.5 plotted against mass density in g/cm^3 , respectively, where straight lines are linear regression lines. For P-waves measured at 10 kbar pressure, Birch (1961) found $\alpha = 3.05\rho - 1.87$ for rocks having mean atomic weight ~ 21 . The relationships among velocity and mass density is called Birch's law. Kanamori and Mizutani (1965) found $\alpha = 2.8\rho - 1.3$ at 6 kbar (0.6 GPa) for dunite, peridotite and eclogite in Japan. Christensen (1968) made laboratory measurements on rocks typical of those suspected to compose the upper mantle and found that S-wave velocity varies as $\beta = 1.63\rho - 0.88$ at 10 kbar for mean atomic weight ~ 22 . Manghnani et al. (1974) measured both P- and S-wave velocities for granulite facies rocks and eclogite and found $\alpha = 2.87\rho - 1.85$ and $\beta = 1.40\rho - 0.33$ at 10 kbar where mean atomic weight ~ 22 .

Christensen and Mooney (1995) reported on laboratory P-wave velocity measurements of many rocks that compose the earth's crust. They grouped the rocks into a total of 29 categories by common rock type. They made measurements using a common laboratory technique on all the rocks at various pressures corresponding

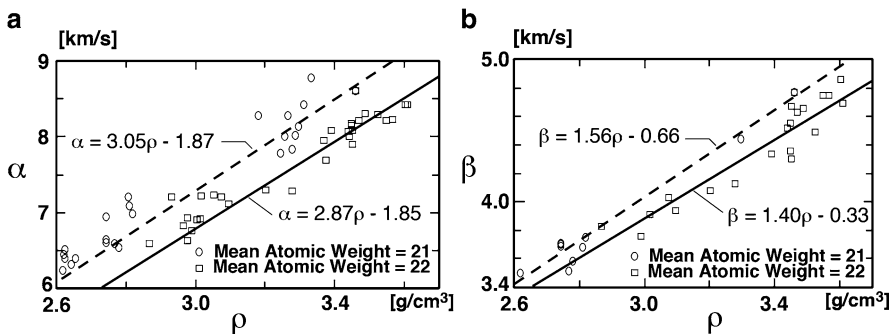


Fig. 2.2 (a) P-wave velocity against mass density and (b) S-wave velocity against mass density for common lithospheric igneous and metamorphic rocks measured at 10 kbar (1 GPa). Dashed lines show fits to data for rocks having mean atomic weights between 20.5 and 21.5 by Birch (1961) for P-waves and Manghnani et al. (1974) for S-waves. Solid lines show fits for rocks having mean atomic weights between 21.5 and 22.5 by Manghnani et al. (1974) for both P- and S-waves. Data from Manghnani et al. (1974) and Birch (1960, 1961)